nature photonics

LETTERS

PUBLISHED ONLINE: 21 NOVEMBER 2016 | DOI: 10.1038/NPHOTON.2016.210

# Ripplon laser through stimulated emission mediated by water waves

Samuel Kaminski, Leopoldo L. Martin*, Shai Maayani and Tal Carmon

**Lasers rely on stimulated electronic transition, a quantum phenomenon in the form of population inversion. In contrast, phonon masers[1–3] depend on stimulated Raman scattering and are entirely classical. Here we extend Raman lasers[1–3] to rely on capillary waves, which are unique to the liquid phase of matter and relate to the attraction between intimate fluid particles. We fabricate resonators that co-host capillary[4] and optical modes[5], control them to operate at their non-resolved sideband and observe stimulated capillary scattering and the coherent excitation of capillary resonances at kilohertz rates (which can be heard in audio files recorded by us). By exchanging energy between electromagnetic and capillary waves, we bridge the interfacial tension phenomena at the liquid phase boundary to optics. This approach may impact optofluidics by allowing optical control, interrogation and cooling[6] of water waves.**

Novel nanolasers[7–9] benefit from using metallic materials. In a similar way, it is possible to exploit different wave systems that extend the concepts of Brillouin lasers[1–3], which rely on acoustical waves, to capillary waves. At a scale smaller than the width of a hair (*capillus* in Latin), the effects that arise from cohesive forces between intimate particles of liquid push to minimize the liquid's surface. Unlike acoustical waves that can propagate in all phases of matter, capillary waves are unique to liquids. Liquid interfaces, such as the ones in a glass of water, tend to be viewed as stationary smooth surfaces that exchange minimal energy with electromagnetic waves. Yet liquid phase boundaries, including those in droplets, actually look like a stormy sea when monitored with Angstrom resolution[10–12] and can therefore scatter and Doppler-shift light. During this scattering process, light can transfer part of its energy to capillary waves through redshift. Scattering from density variations, while coherently generating acoustic waves, is known as a Brillouin laser[1–3]. Raman scattering[1,3] refers to the scattering from fluctuations in charge distribution while the molecule's centre of mass remains stationary. In such scattering processes, energy conservation considerations suggest the stimulated optical generation of coherent oscillations if 'redder' (Stokes) scattering governs over the 'bluer' (anti-Stokes) scattering. Thermodynamically the Boltzmann distribution[13] implies a sufficient Stokes enhancement for Raman and Brillouin lasers[1], as can be seen in Fig. 1. In contrast, capillaries have rates ($10^3$ Hz) much lower than optical frequencies ($10^{14}$ Hz), suggesting that their Stokes and anti-Stokes lines are almost equal. In other words, there will be no optocapillary energy exchange because the Stokes-created ripplons will be balanced by the anti-Stokes-annihilated ripplons. To mitigate this Stokes–anti-Stokes balance, it is possible to 'help' the Boltzmann distribution in the task of enhancing the capillary Stokes line. For example, the Stokes line can be resonantly enhanced (over the anti-Stokes line) by operating at the sideband of an optical resonance (Fig. 1b). Such a usage of sideband control is important in the cooling of gasses[6] and in the excitation of phonon lasers[14]. It would therefore seem that forcing the optical cavity of a liquid droplet[5,15–20] to operate at its non-resolved sideband regime would allow ripplon laser emission. Yet, just as low acoustic attenuation is needed for Brillouin lasers[1–3], low viscosity is required for capillary oscillations. Low-viscosity (runny) liquids are, however, experimentally challenging because of their inherently fast evaporation rates. One recently demonstrated resonator system that is both small and resistant to evaporation uses optical tweezers to submerge a microdroplet near an optical coupler[18]. Here we use this technique[18] to cancel out evaporation, but use runny liquids that transform the system from the capillary overdamped to the capillary underdamped operation regime.

Our hybrid optocapillary resonator is an octane microdroplet in water. Octane and water are chosen here for their low viscosities (0.54 and 1.0 mPa s) and for their high transparency, which allow a capillary quality factor ($Q_{cap}$) of 18 together with an optical quality factor ($Q_{opt}$) of $1 \times 10^6$. When the circumference of the droplets is an integer number of optical wavelengths, an optical whispering gallery mode (Fig. 2a, the arrow along the equatorial line) is possible. The transverse profile of this mode is calculated[21] to reside at the droplet interface (Fig. 2a, inset on the bottom right). Similar to its optical modes, the droplet can also resonate when its size is near an integer number of capillary wavelengths. The eigenfrequencies[22], $f_i$, of the capillary shape oscillations (Fig. 2b) are

$$f_i^2 = \{\gamma\, i(i+1)(i+2)\}/\{4\pi^2 R^3[(i+2)\,\rho_0 + (i+1)\,\rho_w]\} = k/m \quad (1)$$

where $\gamma$ is the surface tension, $R$ is the droplet radius, $\rho_0$ and $\rho_w$ are the mass densities of octane and water and $i$ is the mode order. To give a scale relevant to our experiment, a droplet with $R = 90$ μm, $\rho_w = 1{,}000$ kg m$^{-3}$, $\rho_o = 708$ kg m$^{-3}$ and $\gamma = 13.7$ mJ m$^{-2}$ will have a natural frequency, $f_1$, of 1,664 Hz and an $f_3$ value of 4,767 Hz. Here $m$ and $k$ are the effective mass and spring constant for a given droplet mode[23], and are convenient for describing radius changes of the droplet, $r$, with time using the harmonic oscillator equation[23]

$$m\ddot{r}(t) + b\dot{r}(t) + kr(t) = 2\pi|A(t)|^2/c \quad (2)$$

where $b$ is the damping coefficient, $c$ is the speed of light in the resonator and $|A(t)|^2$ is the optical power circulating in the droplet while its radius is inflated by applying centrifugal radiation pressure. Cavity inflation, $r(t)$, will in return Doppler shift the optical resonance frequency by $\Delta\omega(t)$ as described by[23]

$$\Delta\omega(t) = \Delta\omega_0 - \frac{2\pi\omega\, r(t)}{\lambda N} \quad (3)$$

where $\lambda$ is the optical wavelength in the resonator, $N$ is an integer describing the circumference divided by the resonance wavelength and $\omega$ is the angular optical frequency. $\Delta\omega_0$ is the detuning between the frequency of the optical pump and the cavity resonance frequency

Faculty of Mechanical Engineering, Technion, 32000 Haifa, Israel. *e-mail: llmartin@tx.technion.ac.il



© 2016 Macmillan Publishers Limited, part of Springer Nature. All rights reserved.

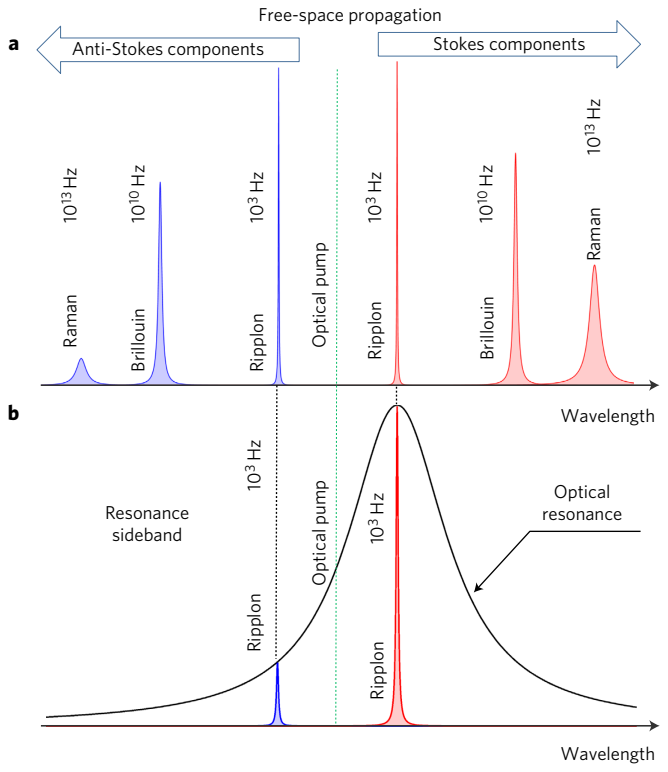


**Figure 1 | Light–matter interactions. a**, In bulk samples, optical and acoustiphonons have rates that are large enough to thermodynamically enhance their Stokes lines to enable Raman and Brillouin lasers. In contrast, the lower frequency of ripplons suggests a Stokes–anti-Stokes balance that makes ripplon lasers challenging. **b**, Mitigating this limitation and tilting this balance to favour Stokes emission can be achieved by working at the non-resolved sideband of an optical resonance.

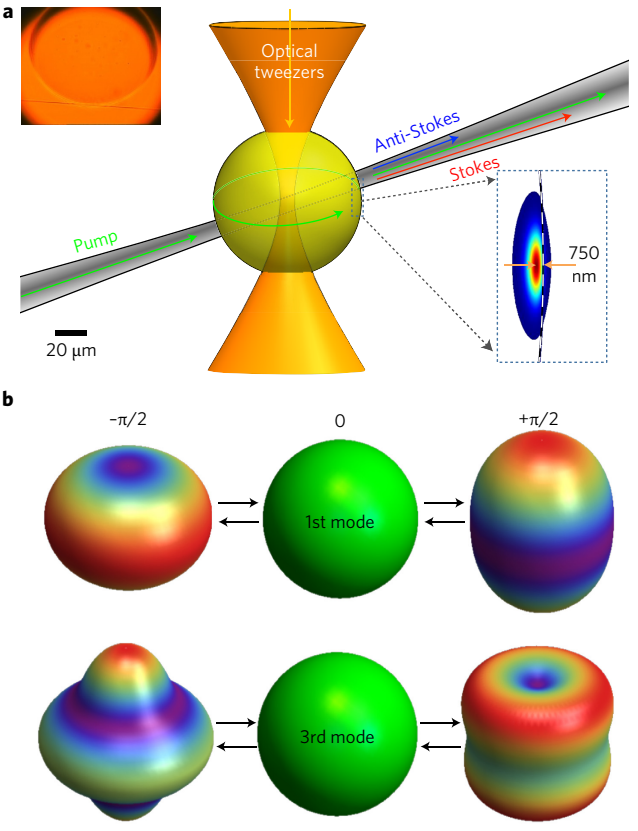


**Figure 2 | Experimental set-up. a**, Optical tweezers (orange) manipulate an octane microdroplet (yellow, see inset image) submerged in water (light blue) near a tapered coupler, from which the microdroplet receives pump light (green). Radiation pressure from circulating light (green ring) excites capillary oscillations giving rise to Stokes radiation. **b**, Droplet capillary resonances where the shape change and colours represent the droplet's deformation (see Supplementary Movies 1 and 2).

while at capillary equilibrium and therefore describes the initial size and sign of the sidebands. The total detuning, $\Delta\omega(t)$, affects the optical field inside the resonator, $A(t)$ (in units of $\sqrt{\mathrm{W}}$) as described by[24]

$$\dot{A}(t) + A(t)[\alpha c - I\Delta\omega(t)] = IB\sqrt{\frac{\alpha c}{\tau_0}} \qquad (4)$$

where $\alpha$ is the optical loss in the cavity (in units of $\mathrm{m}^{-1}$), $B$ is the input pump field, $I = \sqrt{-1}$, and $\tau_0$ is the photon roundtrip time. The solution of this set of coupled differential equations (equations (2)–(4)) will later be compared with our experimental results.

Our main result relates to a self-consistent process in which capillary resonances are excited by light. In return these capillary resonances reflect and Doppler shift the optical pump that turns into a Stokes emission line. To experimentally demonstrate this effect, we slowly scan our 770 nm pump laser through a droplet's optical resonances while we control the droplet–coupler distance using a 532 nm optical tweezers (Fig. 3a). As is common to micro-resonators, the average absorption is shaped like a shark's tail, which originates from thermal effects[25]. Yet unlike in any previous experiment, including those with whispering gallery resonators, a periodic transmission oscillation is measured at a kilohertz rate. As these recorded oscillations (Fig. 2a,e) are at audio rates, one can actually listen to them in a soundtrack that we provide in Supplementary Movies 3–6. Importantly, we finely tune the taper–resonator distance until the amplitude of the transmission oscillations reaches a maximum. This controlled coupling is important in extracting the largest proportion of the Stokes line out of the resonator—commonly referred to as optimal coupling[26]. When optimally coupled (Fig. 3a), we observe strong interference oscillations between the Stokes and pump light with an amplitude that reaches 70% of the transmission, indicating the strength of our Stokes process. To compare the experimental results to the theory, the transmission is calculated using equations (2)–(4) and is presented (Fig. 3b, red) next to the experimental data (Fig. 3b, blue). The parameters in this calculation are $Q_c = 18$ (the capillary $Q$ is defined as $Q_c = (2\pi/\alpha_c\lambda_{cap})$ where $\alpha_c$ is the capillary attenuation and $\lambda_{cap}$ is the capillary wavelength; $\alpha_c$ was calculated using equation (10) from ref. 27) as revealed from the known viscosities and mass densities, and $Q_{opt} = 10^7$, as estimated on the basis of octane transmission.

Fourier-transforming the oscillations shown in Fig. 3a reveals the frequency spectrum (Fig. 3c). The strongest spectral line in Fig. 3c (black line) represents the beatnote between the pump and the Stokes line. This fundamental line is accompanied by its 2nd, 3rd and 4th harmonics (Fig. 3c, grey line), suggesting that multi-ripplon processes are also involved here. For example, the second line in Fig. 3c indicates a process in which two ripplons, each at 1,770 Hz, are created while the pump photons is shifted by $2 \times 1{,}770 = 3{,}540$ Hz. This is usually referred to as a multiphonon Raman process.

In general, self-sustained oscillations arise when a positive feedback is added to a system with characteristic oscillations[11,23,28]. Here, the thermal (Brownian) vibrations of a droplet modulate the intracavity optical power, which reciprocally drives the droplet to oscillate. As expected, and is commonly found in such systems[11,23,26,28],



© 2016 Macmillan Publishers Limited, part of Springer Nature. All rights reserved.

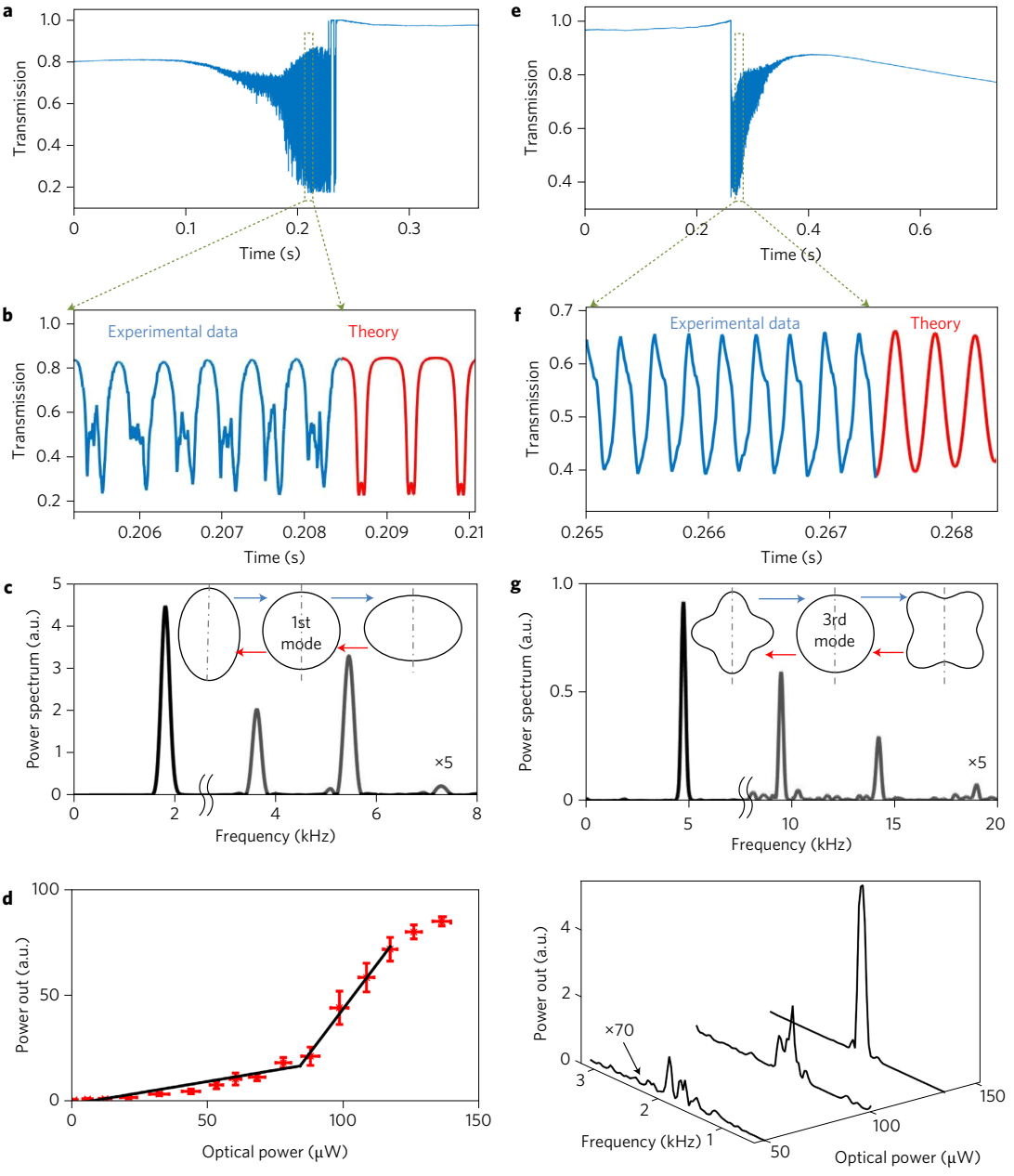


**Figure 3 | Experimental results. a**,**b**, A slow scan of the pump laser wavelength through an optical resonance of a droplet reveals periodic oscillations in optical transmission (**a**,**b**; blue), that are shown next to the theoretically expected variation (red). **c**, The transmission oscillation spectrum is revealed by Fourier transforming **a**. **d**, The amplitude of the periodic oscillations grows with input power (left) with a knee marking the transition from spontaneous scattering by Brownian capillary oscillations to optically excited oscillations. A narrowing of the emission line is measured with increasing pump power (right). Error bars represent standard error. **e**–**g**, On reversing the scan direction the mirrored evolution of oscillations (with respect to **a**) indicates that ripplon lasers always appear at the blue sideband irrespective of the scan direction. The grey lines in **c** and **g** are ×5 magnification of the original magnitude. **e**,**f**, A mode at a different frequency is depicted. Laser wavelength = 770 nm, $R$ = 90 μm, the refractive index = 1.33 for water and 1.4 for octane.

as the input power is increased from zero there is a linear increase in the oscillations, indicating spontaneous scatterings from Brownian capillary-fluctuations. A knee at 77.4 μW (Fig. 3d, left) marks the region where the optical gain becomes equal to the energy loss (including energy lost due to viscosity), which is the power threshold region for oscillation. Theoretically calculating the power threshold using[28]

$$P_{\text{threshold}} = \frac{5R^2\omega^2\sqrt{m\,k}}{32}\,\frac{1}{Q_{\text{opt}}^3\,Q_{\text{cap}}} \qquad (5)$$

with $Q_{\text{opt}} = 3 \times 10^6$ reveals the measured threshold (77.4 μW). Above the threshold power the slope of the curve steepens and then saturates. This indicates optically induced oscillation, followed by reaching the depleted-pump regime; the oscillation linewidth narrows with input power (Fig. 3d, right).

We now repeat this experiment (Fig. 3a–c) while reversing the laser scanning direction. By reversing the scan direction we experimentally verify that oscillations appear at the blue sideband (Fig. 3e) irrespective of the scan direction.

Two eigenfrequencies, one at 1,770 and the other at 4,500 Hz, can be seen in Fig. 3c,g at comparable values to those calculated



© 2016 Macmillan Publishers Limited, part of Springer Nature. All rights reserved.

above (1,664 and 4,767 Hz). With these two experimentally measured frequencies, it is possible to extract a surface tension of $\gamma = 13.7$ mJ m$^{-2}$ using equation (1) (see Methods for more information).

This excitation of different modes (Fig. 2c,g) is typical because higher-optical-quality modes tend to excite oscillations at a lower rate[29]. The absence of the second mode is also typical because even modes tend to have their node near the equator line and therefore have a smaller opto-capillary coupling[28].

Optical excitation and interrogation of the capillary droplet modes suggest that they can host analytes while functioning as a multi-sensory detector with contributions from optical, acoustic[19] and capillary resonances. This is in contrast to multi-spectral sensors, where different frequencies of the same type of wave participate.

Our device also exhibits giant softness because the restoring force here relies on surface tension. This is unlike technologies based on solid materials, where the restoring force relates to the stiffness (Young's modulus). Similar to the ease of pushing a finger against a water interface (in comparison with pushing against solid glass), the softness of our cavity is a million times larger than silica; the deformation of the device by radiation pressure is consequently enhanced. For this reason, the coolability of such a soft device (when the pump is red detuned) can be improved—this may make it possible to reach the ground state at room-temperature conditions using opto-capillary cooling alone.

## Methods

Methods and any associated references are available in the online version of the paper.

Received 7 March 2016; accepted 29 September 2016; published online 21 November 2016

## References


1. Chiao, R., Garmire, E. & Townes, C. in *Proc. Inter. School Phys. Enrico Fermi Course XXXI, Varenna Italy*, 19–31 (1963).
2. Chiao, R. Y., Townes, C. H. & Stoicheff, B. P. Stimulated Brillouin scattering and coherent generation of intense hypersonic waves. *Phys. Rev. Lett.* **12,** 592–595 (1964).
3. Shen, Y. R. & Bloembergen, N. Theory of stimulated Brillouin and Raman scattering. *Phys. Rev.* **137,** A1787–A1805 (1965).
4. Rayleigh, L. *Proc. R. Soc. Lond.* **29,** 71–97 (1879).
5. Ashkin, A. & Dziedzic, J. Observation of resonances in the radiation pressure on dielectric spheres. *Phys. Rev. Lett.* **38,** 1351–1354 (1977).
6. Aspect, A., Arimondo, E., Kaiser, R. E. A., Vansteenkiste, N. & Cohen-Tannoudji, C. Laser cooling below the one-photon recoil energy by velocity-selective coherent population trapping. *Phys. Rev. Lett.* **61,** 826–829 (1988).
7. Noginov, M. *et al.* Demonstration of a spaser-based nanolaser. *Nature* **460,** 1110–1112 (2009).
8. Oulton, R. F. *et al.* Plasmon lasers at deep subwavelength scale. *Nature* **461,** 629–632 (2009).
9. Nezhad, M. P. *et al.* Room-temperature subwavelength metallo-dielectric lasers. *Nat. Photon.* **4,** 395–399 (2010).
10. Mitsui, T. Observation of ripplon on the liquid droplet adhered to the tip of an optical fiber. *Jpn. J. Appl. Phys.* **43,** 6425–6428 (2004).
11. Metzger, C. H. & Karrai, K. Cavity cooling of a microlever. *Nature* **432,** 1002–1005 (2004).
12. Maayani, S., Martin, L. L., Kaminski, S. & Carmon, T. Cavity optocapillaries. *Optica* **3,** 552–555 (2016).
13. Kittel, C. *Introduction to Solid State Physics* (Wiley, 2005).
14. Vahala, K. *et al.* A phonon laser. *Nat. Phys.* **5,** 682–686 (2009).
15. Tzeng, H.-M., Wall, K. F., Long, M. & Chang, R. Laser emission from individual droplets at wavelengths corresponding to morphology-dependent resonances. *Opt. Lett.* **9,** 499–501 (1984).
16. Hossein-Zadeh, M. & Vahala, K. J. Fiber-taper coupling to whispering-gallery modes of fluidic resonators embedded in a liquid medium. *Opt. Express* **14,** 10800–10810 (2006).
17. Jonáš, A., Karadag, Y., Mestre, M. & Kiraz, A. Probing of ultrahigh optical Q-factors of individual liquid microdroplets on superhydrophobic surfaces using tapered optical fiber waveguides. *J. Opt. Soc. Am. B* **29,** 3240–3247 (2012).
18. Kaminski, S., Martin, L. L. & Carmon, T. Tweezers controlled resonator. *Opt. Express* **23,** 28914–28919 (2015).
19. Dahan, R., Martin, L. L. & Carmon, T. Droplets acoustics. *Optica* **3,** 175–178 (2016).
20. Maayani, S., Martin, L. L. & Carmon, T. Water-walled microfluidics makes an ultimate optical finesse. *Nat. Commun.* **7,** 10435 (2016).
21. Oxborrow, M. Traceable 2-D finite-element simulation of the whispering-gallery modes of axisymmetric electromagnetic resonators. *IEEEE Trans. Microw. Theory* **55,** 1209–1218 (2007).
22. Strani, M. & Sabetta, F. Free vibrations of a drop in partial contact with a solid support. *J. Fluid Mech.* **141,** 233–247 (1984).
23. Carmon, T., Rokhsari, H., Yang, L., Kippenberg, T. J. & Vahala, K. J. Temporal behavior of radiation-pressure-induced vibrations of an optical microcavity phonon mode. *Phys. Rev. Lett.* **94,** 223902 (2005).
24. Gorodetsky, M. L. & Ilchenko, V. S. Optical microsphere resonators: optimal coupling to high-Q whispering-gallery modes. *J. Opt. Soc. Am. B* **16,** 147–154 (1999).
25. Carmon, T., Yang, L. & Vahala, K. Dynamical thermal behavior and thermal self-stability of microcavities. *Opt. Express* **12,** 4742–4750 (2004).
26. Milonni, P. W. & Eberly, J. H. *Lasers* 324–327 (Wiley, 1988).
27. Behroozi, F., Smith, J. & Even, W. Stokes' dream: measurement of fluid viscosity from the attenuation of capillary waves. *Am. J. Phys.* **78,** 1165–1169 (2010).
28. Rokhsari, H., Kippenberg, T., Carmon, T. & Vahala, K. J. Radiation-pressure-driven micro-mechanical oscillator. *Opt. Express* **13,** 5293–5301 (2005).
29. Carmon, T. & Vahala, K. J. Modal spectroscopy of optoexcited vibrations of a micron-scale on-chip resonator at greater than 1 GHz frequency. *Phys. Rev. Lett.* **98,** 123901 (2007).


## Acknowledgements

This research was supported by the Israeli Centers of Research Excellenece (ICore) Circle of Light and by the Israeli Science Foundation under grant no. 2013/15.

## Author contributions

S.K. and L.L.M. fabricated the devices and performed the experiments. S.K. and S.M. analysed the data. L.L.M. and T.C. supervised the research.

## Additional information

Supplementary information is available in the online version of the paper. Reprints and permissions information is available online at www.nature.com/reprints. Correspondence and requests for materials should be addressed to L.L.M.

## Competing financial interests

The authors declare no competing financial interests.



© 2016 Macmillan Publishers Limited, part of Springer Nature. All rights reserved.

## Methods

We fabricate optocapilary microdroplet resonators by blending octane, water and a tween-40 emulsifier (14.9, 85 and 0.1%) in an ultrasonic bath. Using a pipette, we then transfer an octane droplet to our experimental set-up (Fig. 2a) where optical tweezers position[18] it near a tapered-fibre coupler[30]. We measured the surface tension for the octane–water–surfactant interface to be 23.6 mJ $m^{-2}$ using the Neumann Triangle method.

Importantly, we fabricated our taper such that the speed of light inside it equals to the speed of light circulating in the resonator. This enables phase-matching that can potentially allow all of the light to couple. During the experiment, we then have a finer control over the speed of light by moving the resonator towards thinner (or thicker) regions of the taper.

As silica tapers are highly hydrophilic, they prefer to be in contact with water rather than the octane resonator. For this reason, we never observed the octane droplet sticking to the silica taper, even when we were intentionally trying cause this.

The droplet is trapped with a 5 mW laser beam passing through a lens with a numerical aperture of one. The center of mass (COM) for the droplet moves in a Brownian manner while trapped by the optical tweezers. Using relations from ref. 5, we calculate the COM motion to be in the order of 5 nm, meaning that such motion can affect transmission by less than 1% (see ref. 31), which is smaller than the ripplon laser-induced changes in transmission (47%, Fig. 3b). The expected eigenfrequency of this droplet COM motion is expected to be near 50 Hz, which is much smaller than the ripplon laser rates (1,770 and 4,500 Hz). Although we did not observe oscillations that originated from the Brownian motion of the droplet COM, we don't exclude the possibility that such oscillations could be measured in the future.

## References

30. Knight, J., Cheung, G., Jacques, F. & Birks, T. Phase-matched excitation of whispering-gallery-mode resonances by a fiber taper. *Opt. Lett.* **22,** 1129–1131 (1997).
31. Little, B. E., Laine, J.-P. & Haus, H. A. Analytic theory of coupling from tapered fibers and half-blocks into microsphere resonators. *J. Lightwave Technol.* **17,** 704–715 (1999).



© 2016 Macmillan Publishers Limited, part of Springer Nature. All rights reserved.